

## Effect of Shot Peening and Pre-Oxidation Duplex Treatment on Electrochemical Corrosion Behavior of Al Alloy in Alkaline Soil

Fengjie Yan<sup>1,2</sup>, Xuegang Wang<sup>3</sup>, Xiaoming Wang<sup>2</sup>, Xingeng Li<sup>2</sup>, Chengguo Wang<sup>1,\*</sup>

<sup>1</sup> School of Materials Science and Engineering, Shandong University, Jinan 250061, China

<sup>2</sup> Material Laboratory of State Grid Corporation of China (Shandong), State Grid Shandong Electric Power Research Institute, Jinan 250001, China

<sup>3</sup> School of Materials Science and Engineering, Linyi University, Linyi 276000, China

\*E-mail: [sduwchg@163.com](mailto:sduwchg@163.com)

Received: 8 August 2017 / Accepted: 26 September 2017 / Published: 12 November 2017

---

The aim of this article was to develop a surface modification process to enhance the corrosion resistance of Al alloy in soil. Shot peening combined with pre-oxidation was conducted to Al alloy and its effects on corrosion behavior of Al alloy in soil were investigated by optical microscopy, scanning electronic microscopy, electrochemical testing and accelerating corrosion test. The results showed that the duplex treatment can refine the grain and second phase ( $\theta$ -Al<sub>2</sub>Cu) in the surface region of Al alloy. Compact and homogenous corrosion products (CuAlO<sub>2</sub> and Al<sub>2</sub>O<sub>3</sub>·3H<sub>2</sub>O) without pitting corrosion were formed on the surface of treated samples. Compared to the as-received sample, surface treatment can reduce the corrosion current density and increase the impedance value, indicating an excellent corrosion resistance. The running experiment of 60 days showed that Al alloy with surface treatment can be used as a grounding material with excellent anti-corrosion in soil.

---

**Keywords:** Al alloy grounding material; pitting corrosion; shot peening; pre-oxidation; soil corrosion

### 1. INTRODUCTION

Grounding grid is designed to ensure safety of personnel and equipment in reliable operation of power system [1, 2]. When the power equipments is suffered from short circuit or lightning, grounding grid should provide enough capacity for high fault current to dissipate it in the soil [3-4]. So good grounding conductivity, thermal stability performance and anti-corrosion in soil are the basic requirements for grounding materials [5]. Pure Al is generally not allowed as grounding material for its corrosion products of Al<sub>2</sub>O<sub>3</sub> and Al (OH)<sub>3</sub> in the soil have poor conductivity and will result in high grounding resistance. Adding copper in Al alloy can improve its grounding conductivity due to the

formation of  $\text{CuAlO}_2$  oxide film. However, the intermetallic compounds of  $\text{Al}_2\text{Cu}$  cannot be avoided when adding copper to Al matrix and will reduce the resistance corrosion in the soil. In our previous research, a novel Al alloy was developed to meet the electrical performance requirements and anti-corrosion performance by obtaining  $\alpha$  solid solution matrix and a small amount of  $\text{Al}_2\text{Cu}$  phase structure. However, when the Al alloy grounding material is used in alkaline soil with high chloride ion, it is prone to pitting corrosion and intergranular corrosion due to the erosion of chloride ions and the cathodic behavior of  $\text{Al}_2\text{Cu}$  with respect to the base alloy. Hence, it is important to study the corrosion behavior of Al alloy grounding material and to improve its corrosion resistance using appropriate surface treatment methods.

Shot peening is an important technique to enhance corrosion resistance. Several studies have been carried out about the effect of shot peening on the microstructure and corrosion behavior of stainless steel [6-8]. Peyre found that shot peening had a beneficial influence on localized corrosion properties of stainless steel by changing the microstructure. Wang [9] pointed out that high-energy shot-peening induced the nanocrystalline microstructure in the surface of 1Cr18Ni9Ti stainless steel. The surface nanocrystallization can markedly enhance the corrosion resistance of 1Cr18Ni9Ti stainless steel in the chlorine-ion-contained solution. According to Chen [10], machine hammer peening had a beneficial influence on the corrosion resistance of nickel-base alloy 718 due to the formation of nano-grains and nano-twins. Zupanc and Mhaede [11, 12] reported that shot-peening treatment had a favorable influence on corrosion fatigue properties of Al alloy by inducing compressive residual stresses and local plastic deformations.

Pre-oxidation is also an effective surface modification technique to affect the alloy corrosion properties by modifying the surface passive/oxide film and the surface microstructure [13-15]. Barranco [16] found that thermal oxidation treatments decreased the susceptibility to pitting corrosion of blasted  $\text{Ti}_6\text{Al}_4\text{V}$ .

From the literature review, it can be guessed that both of shot peening and pre-oxidation for appropriate process parameter exhibit positive effect on metal corrosion resistance. However, few studies have been carried out on the effect of surface modification treatment on corrosion behavior of Al alloy in soil. The aim of this research was to investigate the effect of shot peening combined with pre-oxidation on the microstructure and the corrosion behavior of Al alloy in alkaline soil.

## 2. EXPERIMENTAL

### 2.1. Material preparation

The experiment materials included pure Al, pure Cu, galvanized steel and Al alloy which contained (in mass %) 4.61Cu, 0.12La, 0.08Ce and Al. The samples were firstly treated by shot peening and then treated by pre-oxidation. Before shot peening, an annealing of  $365^\circ\text{C}$  for 1 hour was conducted. Shot peening was conducted using 60# glass beads by compressed air. The parameters of shot peening were listed in table 1. The pre-oxidation was performed at  $400^\circ\text{C}$  for one hour in a heat treatment furnace.

Samples for accelerated corrosion experiment were cut to 50mm×30mm×5mm and then cleaned ultrasonically in acetone and rinsed with alcohol. Samples for electrochemical experiment were cut to 10mm×10mm×5mm and cleaned ultrasonically in acetone. An exposure area of 1 cm<sup>2</sup> was prepared by mounting with epoxy resin.

**Table 1.** Parameters of shot peening.

Wheel abrator size, /mm	Compressed air pressure /MPa	Shot feed/ kg·min <sup>-1</sup>	Wheel abrator feed / mm·min <sup>-1</sup>	Cyclic times
Φ6×120	0.10	0.30	500	2

### 2.2. Experimental medium preparation

Test medium was soil and soil extract. Soil was taken from 0.8m underground. The soil was ground, passed through a 20-mesh sieve and dried in an oven for six hours. The soil extract was obtained by mixing 1000ml of deionized water with 200g of dry soil and then filtering out the soil. Some selected physical and chemical properties of the soil were summarized in Table 2.

**Table 2.** Physical and chemical properties of soil (mass%).

Ca <sup>2+</sup>	Mg <sup>2+</sup>	K <sup>+</sup>	Na <sup>+</sup>	Cl <sup>-</sup>	SO <sub>4</sub> <sup>2-</sup>	NO <sub>3</sub> <sup>-</sup>	HCO <sub>3</sub> <sup>-</sup>
0.0415	0.0124	0.0046	0.1118	0.0918	0.0209	0.0052	0.2733
pH value		Conductivity of soil leaching solution		Conductivity of clay coating			
(1:2.5)		(μS/cm 1:5)		(μS/cm 1:2.5)			
9.23		885.000		536.000			

### 2.3. Experiment methods

Electrochemical measurements were performed through a PARASTAT2273 electrochemical workstation, with Al alloy as the working electrode (WE), a saturated calomel electrode as the reference electrode (RE) and a platinum plate electrode as the counter electrode (CE). All electrochemical tests were conducted in soil extract. Polarization curves of the samples were measured potentiodynamically from -250 mV to 250 mV vs. open-circuit potential (OCP) at a scan rate of 0.333 mVs<sup>-1</sup>. EIS measurements were carried out at corrosion potential in the frequency range of 500 kHz-100 mHz, with a 10mV amplitude signal. EIS were analyzed with ZSimpwin software. All the measurements were conducted at room temperature.

A materials accelerating corrosion test system was employed to carry out the accelerated corrosion test. Test medium was soil with water content from 19% to 21%. The soil moisture content was kept through intermittent spraying deionized water. The soil temperature was kept at 60°C over the test. Test period was 60 days. After finishing the test, the samples were dug out from the test soil

and then cleared with distilled water, and dehydrated using absolute ethyl alcohol. The micro morphology of the corrosion products were analyzed by SEM, EDS and XRD.

The grounding resistances of various grounding materials were compared by the resistances R. The resistances R were measured through a grounding resistance measurement instrument. The measurements were performed by a two electrode system with the sample as one electrode, a metal container as another electrode. The soil medium was filled into the metal container. The samples were uniformly buried in the soil. A certain gap between the samples and the metal container were designed. The resistances R were periodically measured over the accelerating corrosion test course.

### 3. RESULTS

#### 3.1. Microstructure

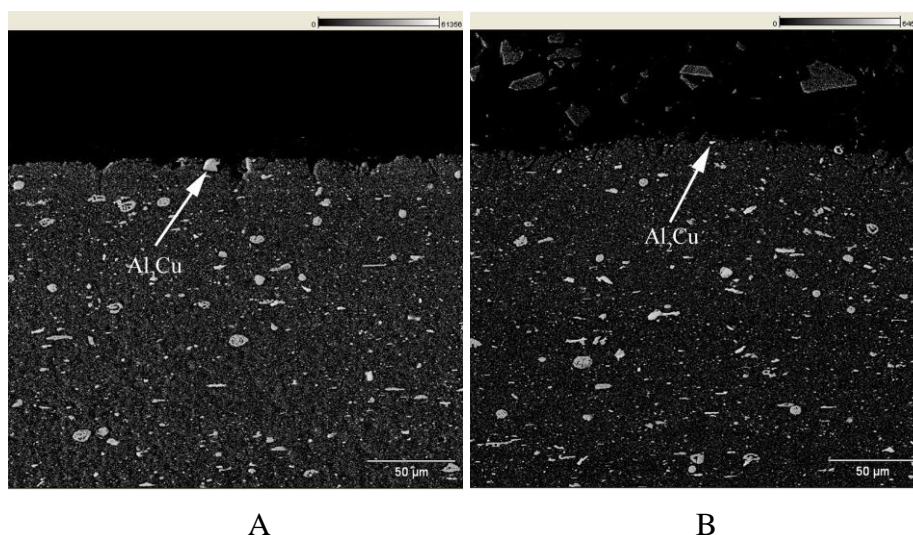


**Figure 1.** SEM images of cross-sectional appearance for Al alloy samples: (a) as-received; (b) shot peening and pre-oxidation.

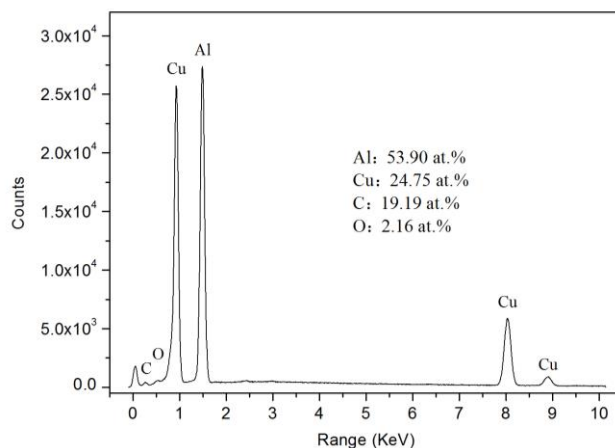


**Figure 2.** EDS spectrum of the coarse second phase particle.

The cross-sectional microstructures of the as-received and treated samples before corrosion are shown in Fig.1. Some second phase particles are found in both samples. The EDS elemental analyses indicate that the second phases are  $\text{Al}_2\text{Cu}$ , as shown in Fig.2. The  $\text{Al}_2\text{Cu}$  phase particles for the as-received samples appear large and uniform. The  $\text{Al}_2\text{Cu}$  phase particles of surface region for the treated samples are finer than those of the as-received samples, which indicate that surface modification treatment can refine the surface second phase particles.

The OM images of the surface region for the samples with and without surface treatment before corrosion are shown in Fig.3. The size of the cross sectional grains for the as-received samples are approximately  $10\mu\text{m}$ . After the surface modification treatment, the sizes of the grains are dramatically decreased to between 1 and  $3\mu\text{m}$  in the surface region. This indicates that surface modification can also refine the grain of Al alloy.

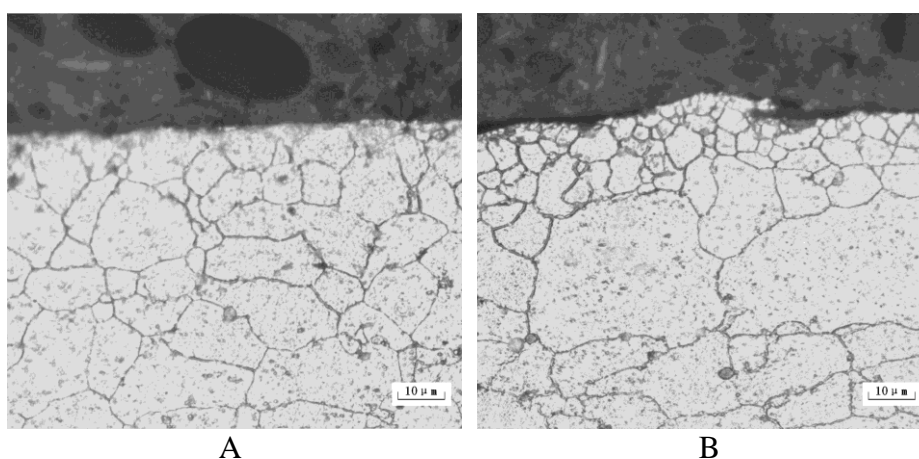


**Figure 3.** OM images of cross-sectional microstructure for Al alloy samples: (a) as-received; (b) shot peening and pre-oxidation.

## 3.2. Corrosion behavior

### 3.2.1 Potentiodynamic polarization

Fig. 4 shows the polarization curves of Al alloy in alkaline soil extract. The Tafel slope and corrosion current density ( $i_{\text{corr}}$ ) are calculated by the Tafel extrapolation method as shown in Table 3. The cathodic Tafel slopes ( $b_c$ ) is much larger than the anodic Tafel slopes ( $b_a$ ), which indicates that the corrosion is controlled by the cathode reaction. The Tafel slopes ( $b_c$  and  $b_a$ ) of the surface treated sample are similar to that of the as-received sample. The  $b_a$  value has a slight decrease due to shot peening increasing the surface energy. Although the anodic reaction is accelerated in the initial stage, but soon a compact corrosion products layer is formed, which blocks the diffusion of oxygen and inhibits the cathodic reaction. The cathodic curve of the surface treated sample shows an obvious left shift relative to the as-received sample, which indicates that the cathodic reaction is inhibited after surface treatment. The anodic curve of the surface treated sample is smooth and shows some passive behavior at the later stage of polarization. However, the anodic curve of the as-received sample

appears some small current fluctuations, indicating an evidence of pitting corrosion [17]. The corrosion currents density ( $i_{corr}$ ) of the sample without and with surface treatment were  $1.003 \times 10^{-6} \text{ A}\cdot\text{cm}^{-2}$  and  $2.409 \times 10^{-7} \text{ A}\cdot\text{cm}^{-2}$ , respectively. The low current density reflects a lower corrosion rate. The results of the polarization cure test indicated that surface treatment remarkably reduced cathodic reaction, improved passivation behavior, inhibited pitting and decreased corrosion rate of Al alloy in alkaline soil extract.

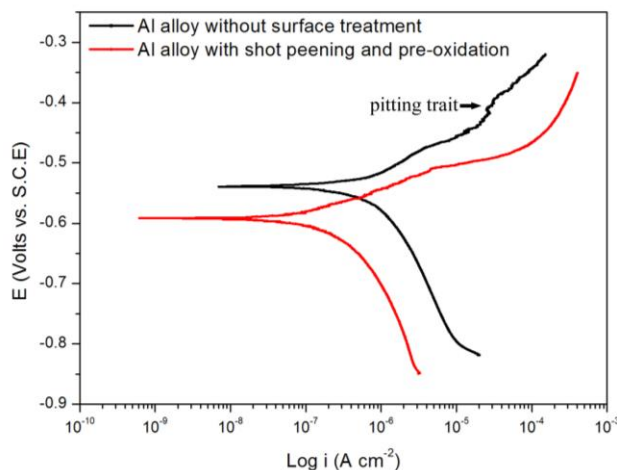


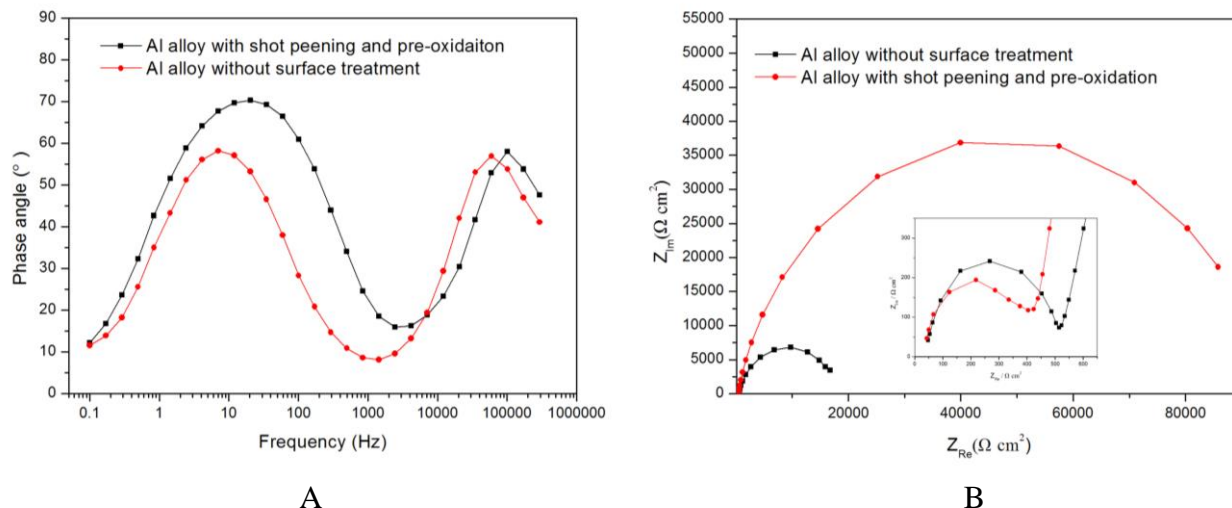
**Figure 4.** Polarization curves of Al alloy in alkaline soil extract.

**Table 3.** Fitted tafel curves results for Al alloy samples measured in soil extract.

sample	$E_{corr}/\text{mV}$	$I_{corr}/\text{A}\cdot\text{cm}^{-2}$	$b_a/\text{mV}\cdot\text{dec}^{-1}$	$b_c/\text{mV}\cdot\text{dec}^{-1}$
Shot peening combined with pre-oxidation	-590	$2.41 \times 10^{-7}$	62	214
As-received	-539	$1.00 \times 10^{-6}$	78	223

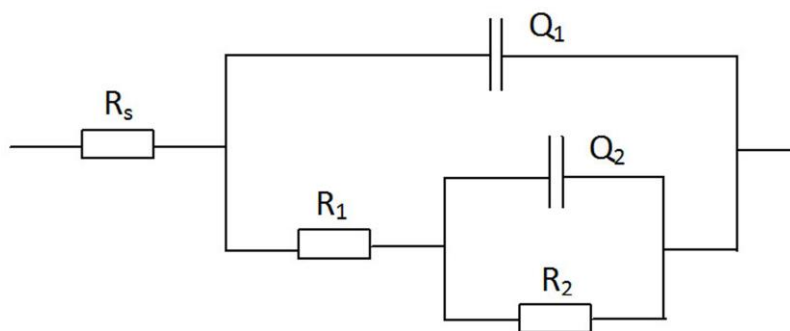
### 3.2.2. Electrochemical impedance spectroscopy

Fig. 5 shows EIS plots of Al alloy in soil extract in the initial stage of corrosion. It is seen that there were two time constants for all plots, identified as two maximum in phase angle plots in the whole measured frequency range, as shown in Fig. 5(a). Two capacitive circles were observed for all plots in the Fig. 5(b), which indicated that the interface reactions were prevented effectively because of the passive film formed on the samples surface. The two EIS plots show qualitatively the same shapes and features in the high-frequency region. However, in the low-frequency region, the impedance modulus of the surface treated sample is significantly higher in comparison with that of the as-received sample.



**Figure 5.** Nyquist and bode plots of Al alloy in alkaline soil extract: (a) Bode plots; (b) Nyquist plots.

EIS can reflect the majority of electrochemical characteristics as well as some physical processes of a corrosion system. The kinetic parameters of electrochemical reactions in corrosion processes can be obtained by analyzing EIS plots. According to some reference as reported by Luo [18], a model had been selected for the Al alloy sample. The equivalent circuit consists of the solution resistance  $R_s$  connected in series with two time constants  $R_1[Q_1(R_2Q_2)]$ . The two R-Q elements equivalent circuit in Fig. 6 was adopted to fit the experimental data. There is a good agreement with the equivalent circuit predictions and the experimental data. The high-frequency capacitive loop is caused by a charge transfer resistance ( $R_1$ ) in parallel with a double-layer capacitance ( $Q_1$ ). At lower frequencies, the parameter  $Q_2$  represents the capacitive behavior of the passive film formed, coupled with a resistance ( $R_2$ ) due to the ionic paths through the oxide film. The fitted impedance parameters are summarized in Table 4. It is observed that the values of the two  $R_2$  are much higher than  $R_1$ , which means that the protection of the passive film is the control factor of corrosion reaction. As compared with the as-received Al alloy sample, the treated sample shows a higher  $R_2$ , which suggests that the passive film formed on the surface of the treated sample is denser and more protective than the one did on the as-received Al alloy sample.



**Figure 6.** Circuit model of Al alloy in alkaline soil extract.

**Table 4.** Fitted EIS results for Al alloy samples measured in soil extract.

sample	$R_s/\Omega\text{cm}^2$	$Q_1/\Omega^{-1}\text{cm}^{-2}\text{s}^{-n}$	$n_1$	$R_1/\Omega\text{cm}^2$	$Q_2/\Omega^{-1}\text{cm}^{-2}\text{s}^{-n}$	$n_2$	$R_2/\Omega\text{cm}^2$
Shot peening combined with pre-oxidation	33.5	$1.894 \times 10^{-8}$	0.80	385.5	$3.04 \times 10^{-6}$	0.86	$9.32 \times 10^4$
As-received	42.5	$2.386 \times 10^{-6}$	0.97	479.2	$1.304 \times 10^{-5}$	0.84	$1.753 \times 10^4$

3.2.3. Cross-section corrosion morphology

As shown in Fig. 7a and c, the cross section morphology of the surface treated sample is homogeneous whereas the morphology of the as-received sample appears a lot of pitting and intergranular corrosion. The EDS elemental analyses (Fig. 7b and d) of the selected areas from cross section of the samples (Fig. 7a and c) indicate that the surface layer of the as-received sample contains Al, Cu, S, Cl and O, while the surface layer of the treated sample only comprises Al, Cu, O, C and Si. The Si is the element of soil that remains on the surface of the sample. The cross-sectional corrosion appearances of Al alloy after exposure in the soil for 60 days show that the surface treated sample exhibits better corrosion resistance than the as-received sample.

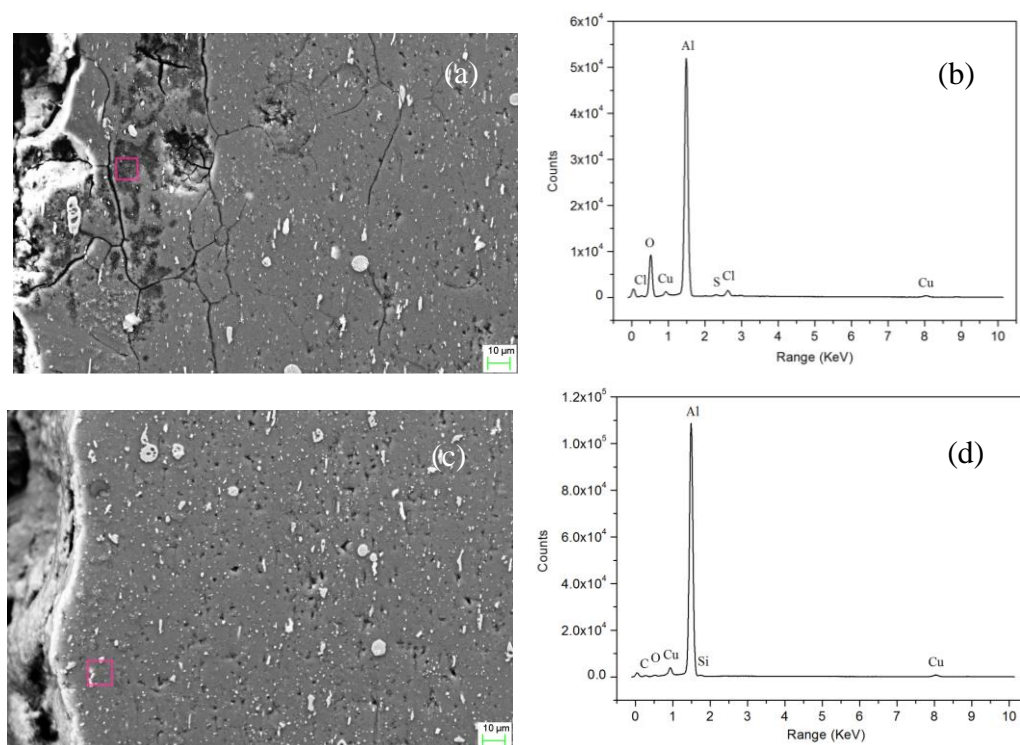


**Figure 7.** SEM cross-sectional micrographs and EDS composition profiles of Al alloy exposed in alkaline soil for 60 days: (a and b) as-received, (c and d) shot peening and pre-oxidation.

### 3.2.4. Surface corrosion morphology and corrosion products

Fig.8 shows the surface morphology of Al alloy samples after accelerating corrosion experience. The image shows that granular corrosion products are observed, which are uniform, tiny and dense, on the surface of treated sample. However, on the surface of as-received sample no granular corrosion products are observed. The results show that shot peening and pre-oxidation cause the corrosion products fine.

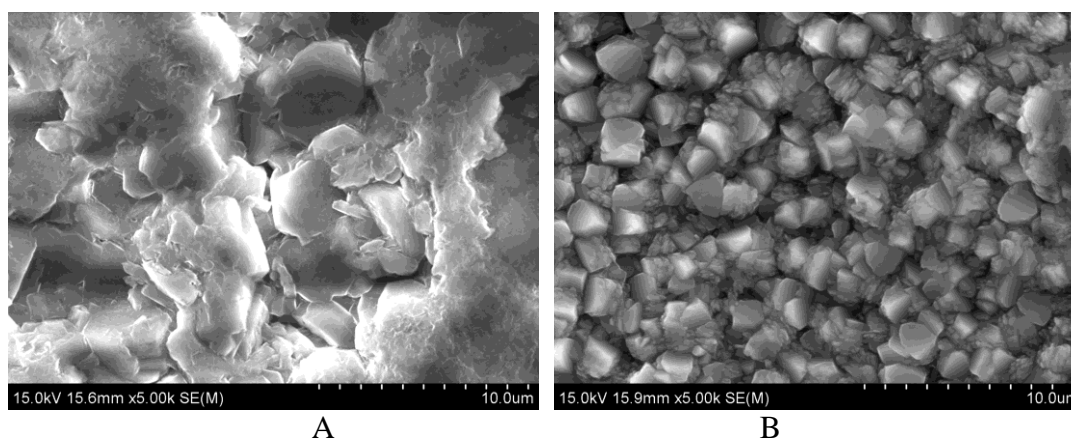


**Figure 8.** Microscopic corrosion appearance of Al alloy exposed in alkaline soil for 60 days: (a) as-received; (b) shot peening and pre-oxidation.

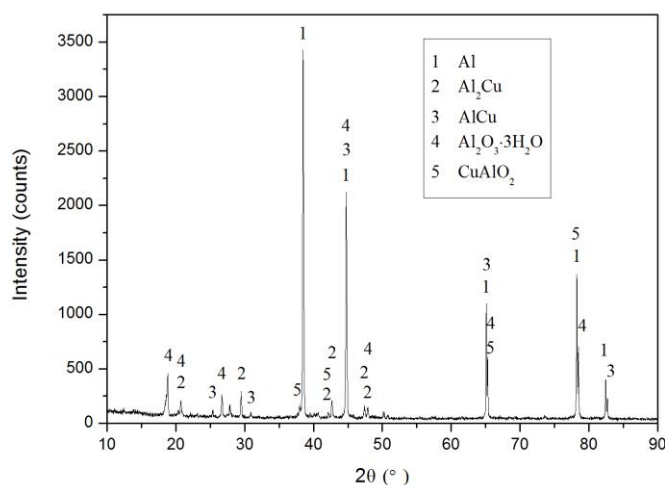


**Figure 9.** XRD patterns of corrosion products and metallic substrate of Al alloy with shot peening and pre-oxidation.

The corrosion products and metallic substrate of surface treated Al alloy were characterized by means of X-ray diffraction (XRD). A step-scanning X-ray diffractometer was used, with Cu  $K\alpha$  radiation, in the scanning range 10-90°. The result revealed that corrosion products consisted of  $\text{Al}_2\text{O}_3 \cdot 3\text{H}_2\text{O}$  and  $\text{CuAlO}_2$ .  $\text{CuAlO}_2$  is transparent conducting oxides and has good conductivity [19], so

the corrosion products have lower grounding resistance. The result of XRD shows that Al alloy matrix contains  $\text{Al}_2\text{Cu}$  and AlCu phases. However, no AlCu phase was found by EDS test on the segregated phases, which indicated that AlCu phase is evenly distributed in the Al matrix. So the corrosion products of compact and homogenous  $\text{CuAlO}_2$  and  $\text{Al}_2\text{O}_3 \cdot 3\text{H}_2\text{O}$  were formed on Al alloy surface in alkaline soil.

### 3.3. grounding conductivity performance

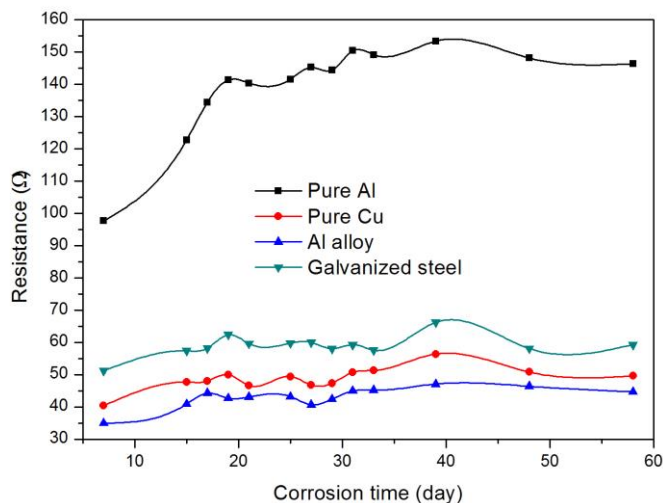


**Figure 10.** Dynamic resistances of the samples exposed in the accelerating corrosion test system for 60d.

Fig.10 shows the resistances  $R$  of four grounding materials over the accelerating corrosion test course. The resistance  $R$  is composed of grounding resistance  $R_1$ , soil resistance  $R_2$  between the metal container and the sample, touch resistance  $R_3$  of the metal container and the soil, and the metal container resistance  $R_4$ . The values of  $R_2$ ,  $R_3$  and  $R_4$  for four grounding material samples are equal respectively by designing the same gap between the samples and the metal container. So we can compare the grounding resistance using the  $R$ . It is clear that the dynamic resistance  $R$  of Al alloy is the lowest among four grounding materials. So the grounding conductivity performance of Al alloy is the best. And it is obviously much better than pure Al. As grounding material, Al alloy can meet the requirement of grounding resistance.

## 4. DISCUSSION

Chloride ion can destroy the metal oxide film and accelerate the anodic reaction of the metal corrosion in soil. It is one of the highly corrosive anions. Chloride ion can penetrate the thin metal oxide layer, and react with metal substrate to form soluble corrosion products. Table 2 shows that the content of chloride ion in test soil is high, which is the main reason for Al alloy pitting. The predominant second phase of Al alloy is  $\text{Al}_2\text{Cu}$  ( $\theta$  phase). The  $\theta$  phase is noble with respect to the aluminum matrix. The noble  $\theta$  phase leads to microgalvanic interactions that cause corrosion of the

surrounding matrix. This is another reason for Al alloy corrosion. The results of the microstructure analysis show that the duplex treatments of shot peening and pre-oxidation refine the grain and second phase. The refinement of metal crystal grains is beneficial to inhibit the damage of the chloride ion [20-22]. Chen [23] found that nanocrystallization could decrease the adsorption ability of  $\text{Cl}^-$  on the surface of the material. Meng [24] reported that passive film formed on nano-scale twins coating was more integrated and more compact than those on industrial electrodeposited nickel. And Meng [25] found that microcrystallization could enhance the repassivation of pure Al and decrease its pitting susceptibility. The works of Ralston and Gupta show that the fine of second phase particles has a positive effect on Al alloy corrosion resistance [26, 27]. The fine of the  $\theta$  phase decreases the cathode reaction area which reduces the microgalvanic interactions. In addition, the fine of second phase leads to a reduction of defects on the surface oxide film as outlined by Ralston [26].

Shot peening can improve the surface energy of alloy which leads to reaction more easily. Shot peening can create surface defects, such as dislocation, void, etc [7]. It is known that the crystal nucleuses of the electrode reaction products are formed firstly in the surface defects. The increase of surface defects leads to the increase of nucleation density. The oxide film of Al alloy formed in the natural environment is amorphous, thin and porous. However, the structure of the oxide film obtained by heating is related with the temperature. The thickness of the oxide film obtained at 400~600°C is 10 times the thickness of the oxide film obtained at room temperature [28]. Under the combined effect of shot peening and pre-oxidation, a fine, dense and uniform oxide film was formed on the surface of Al alloy, which can inhibit the chloride ion and oxygen to penetrate into the matrix. On another hand, the improvement of surface energy and nucleation density also lead to the formation of compact and homogeneous corrosion products in the accelerating corrosion test, which improves the barrier of the chloride and oxygen diffusion, and effectively restrains the pitting of Al alloy. And the fine of corrosion products improves the toughness of the film and the bonding strength between the substrate and film.

## 5. CONCLUSIONS

In this study, surface treatments using shot peening followed by pre-oxidation were carried out on Al alloy in order to improve its corrosion resistance. The effect of shot peening and pre-oxidation on the modification of microstructure and corrosion properties of Al alloy has been characterized. Based on the results obtained in this work, the following conclusions can be drawn.

- (1) Duplex treatment refined the grain and  $\text{Al}_2\text{Cu}$  phase surface region of Al alloy.
- (2) The electrochemical results show that a low corrosion current density and high impedance value was observed. No pitting trait was found.
- (3) Duplex treatment inhibited pitting corrosion and improved the corrosion resistance of Al alloy in soil. This improvement is mainly attributed to the formation of compact and homogenous corrosion products, which forms an adherent barrier layer to inhibit the harm of the anions on the metal matrix.

## ACKNOWLEDGEMENTS

This work is supported by State Grid Corporation of China (No. 2010A-19).

## References

1. M. Bashir, J. Sadeh, E. Kamyab and H. Yaghibi, *Environment and Electrical Engineering (EEEIC), 2012 11th International Conference*, 32(2012 Suppl 1)1022.
2. F.J. Yan, X.G. Li and X.G. Wang, *Applied Mechanics and Materials*, 331 (2013) 416.
3. R. Zeng, X.H. Gong, J.L. He, B. Zhang and Y.Q. Gao, *IEEE Transactions on Power Delivery*, 23(2008)667.
4. S.C. Lim, C. Gomes and M.Z.A.A. Kadir, *Electrical Power and Energy Systems*, 47 (2013) 117.
5. IEEE Guide for Safety in AC Substation Grounding, IEEE Std 80-2000, (2000)192.
6. P. Peyre, X. Scherpereel, L. Berthe, C. Carboni, R. Fabbro, G. Be'ranger and C. Lemaitre, *Materials Science and Engineering A*, 280 (2000) 294.
7. X. G. Li and J. W. He, *Materials Letters*, 60(2006) 339.
8. H. Lim, P. Kim, H. Jeong and H.S. Jeong, *Journal of material Processing Technology*, 212(2012) 1347.
9. T.S. Wang, J.K. Yu and B.F. Dong, *Surface & Coatings Technology*, 200 (2006) 4777.
10. T. Chen, H. John, J. Xu, Q. Lu, J. Hawk and X. Liu, *Corrosion Science*, 77 (2013) 230.
11. U. Zupanc and J. Grum, *Journal of Materials Processing Technology*, 210 (2010) 1197.
12. M. Mhaede, *Materials and Design*, 41 (2012) 61.
13. J.C. Gomez-vidala, A.G. Fernandez, R. Tirawat, C. Turchi and W. Huddleston, *Solar Energy Materials & Solar Cells*, 166 (2017) 222.
14. A. Golshirazi, M. Kharaziha and M.A. Golozar, *Carbohydrate Polymers*, 167 (2017) 185.
15. J.F. Zhgang, X.X. Gan, H.Q. Tang and Y.Z. Zhan, *Materials Science and Engineering C*, 76 (2017) 260.
16. V. Barranco, E. Onofre, M.L. Escudero and M.C. Garcia-alonso, *Surface & Coatings Technology*, 204 (2010) 3783.
17. Y.M. Tang, Y. Zuo and H. Zhao, *Applied Surface Science*, 243(2005)82.
18. H. Luo, C.F. Dong, X.G. Li and K. Xiao, *Electrochimica Acta*, 64(2012)211.
19. C.L. Jiang, Q.J. Liu, F.S. Liu and Z.T. Liu, *Current Applied Physics*, 17(2017) 126.
20. G.Z. Meng, Y.W. Shao, T. Zhang, Y. Zhang and F.H. Wang, *Electrochimica Acta*, 53 (2008) 5923.
21. F.L. Sun, G.Z. Meng, T. Zhang, Y.W. Shao, F.H. Wang, C.F. Dong and X.G. Li, *Electrochimica Acta*, 54(2009)1578.
22. X.Y. Wang and D.Y. Li, *Electrochimica Acta*, 47 (2002) 3939.
23. T. Chen, H. John, J. Xu, Q. Lu, J. Hawk and X. Liu, *Corrosion Science*, 77 (2013) 230.
24. G.Z. Meng, F.L. Sun, Y.W. Shao, T. Zhang, F.H. Wang, C.F. Dong and X.G. Li, *Electrochimica Acta*, 55(2010)2575.
25. G.Z. Meng, L.Y. Wei, T. Zhang, Y.W. Shao, F.H. Wang, C.F. Dong and X.G. Li, *Corrosion Science*, 51 (2009) 2151.
26. K.D. Ralston, N. Birbilis, M.K. Cavanaugh, M. Weyland, B.C. Muddle and R.K.W. Marceau, *Electrochimica Acta*, 55 (2010) 7834.
27. R.K. Gupta, N.L. Sukiman, M.K. Cavanaugh, B.R.W. Hinton, C.R. Hutchinson and N. Birbilis, *Electrochimica Acta*, 66 (2012) 245.
28. Z.F. Zhu. Application handbook of aluminum alloy anodic oxidation process [M]. *Metallurgical Industry Press*, Beijing, China, (2007) 6.